

 Open access • Journal Article • DOI:10.1002/JOC.3522

## SST–convection relation over tropical oceans — [Source link](#)

T. P. Sabin, C. A. Babu, P. V. Joseph

**Institutions:** Indian Institute of Tropical Meteorology, Cochin University of Science and Technology

**Published on:** 01 May 2013 - International Journal of Climatology (John Wiley & Sons, Ltd.)

**Topics:** South Pacific convergence zone, Sea surface temperature, Intertropical Convergence Zone, Convergence zone and Convection

Related papers:

- [Ocean–atmosphere coupling over monsoon regions](#)
- [Sea Surface Temperature, Surface Wind Divergence, and Convection over Tropical Oceans](#)
- [Changes in the sea surface temperature threshold for tropical convection](#)
- [Global analyses of sea surface temperature, sea ice, and night marine air temperature since the late nineteenth century](#)
- [The ERA-Interim reanalysis: configuration and performance of the data assimilation system](#)

Share this paper:    

View more about this paper here: <https://typeset.io/papers/sst-convection-relation-over-tropical-oceans-1ro0qzyrbp>

# SST–convection relation over tropical oceans

T. P. Sabin<sup>a</sup>, C. A. Babu<sup>b</sup> and P. V. Joseph<sup>b\*</sup>

<sup>a</sup> Centre for Climate Change Research, Indian Institute of Tropical Meteorology, Pune, India

<sup>b</sup> Department of Atmospheric Sciences, Cochin University of Science and Technology, Cochin, India

**ABSTRACT:** According to current knowledge, convection over the tropical oceans increases with sea surface temperature (SST) from 26 to 29 °C, and at SSTs above 29 °C, it sharply decreases. Our research shows that it is only over the summer warm pool areas of Indian and west Pacific Oceans (monsoon areas) where the zone of maximum SST is away from the equator that this kind of SST–convection relationship exists. In these areas (1) convection is related to the SST gradient that generates low-level moisture convergence and upward vertical motion in the atmosphere. This has modelling support. Regions of SST maxima have low SST gradients and therefore feeble convection. (2) Convection initiated by SST gradient produces strong wind fields particularly cross-equatorial low-level jetstreams (LLJs) on the equator-ward side of the warm pool and both the convection and LLJ grow through a positive feedback process. Thus, large values of convection are associated with the cyclonic vorticity of the LLJ in the atmospheric boundary layer. In the inter-tropical convergence zone (ITCZ) over the east Pacific Ocean and the south Pacific convergence zone (SPCZ) over the west Pacific Ocean, low-level winds from north and south hemisphere converge in the zone of maximum SST, which lies close to the equator producing there elongated bands of deep convection, where we find that convection increases with SST for the full range of SSTs unlike in the warm pool regions. The low-level wind divergence computed using QuikSCAT winds has large and significant linear correlation with convection in both the warm pool and ITCZ/SPCZ areas. But the linear correlation between SST and convection is large only for the ITCZ/SPCZ. These findings have important implications for the modelling of large-scale atmospheric circulations and the associated convective rainfall over the tropical oceans. Copyright © 2012 Royal Meteorological Society

**KEY WORDS** sea surface temperature and its gradient; atmospheric deep convection; warm pool; ITCZ and SPCZ; low-level jetstreams

Received 27 December 2007; Revised 3 February 2011; Accepted 28 April 2012

## 1. Introduction

The relationship between sea surface temperature (SST) and large-scale convection has been studied in a variety of contexts during the 1960s and 1970s. One important aspect of the character of deep convection revealed through such studies is that it generally occurs more frequently and with more intensity as SSTs become higher (e.g. Bjerknes, 1966, 1969). According to Gadgil *et al.* (1984), organized convection over the tropical Indian ocean occurs when SSTs exceed a threshold or critical value ( $T_c$ ), but once the threshold is crossed, the intensity of convection is no longer dependent on the SST. Graham and Barnett (1987) while confirming this finding for the Pacific and Atlantic oceans found that when SSTs are above  $T_c$ , surface wind divergence is closely associated with convection. It was also found that areas of persistent divergent surface flow coincide with regions where convection appears consistently suppressed even when SSTs are above  $T_c$ .

Studying data from the global tropics, Waliser *et al.* (1993) found that the characteristic of the relationship

between SST and deep convection is such that at temperatures between 26 and 29 °C, convection increases with increasing SST, but above 29 °C, the intensity of convection observed tends to decrease with increasing SST. They found that maximum convective activity does not occur over the warmest ocean but rather the warmest SST occurs under clear or less convective skies. The SST–convection relation found by them (hereafter called the Waliser type) using monthly mean SST data  $2^\circ \text{ lat} \times 2^\circ \text{ lon}$  squares of the entire global tropical oceans and monthly mean convection in the same bins represented by highly reflective clouds (HRCs) and outgoing longwave radiation (OLR) are given in Figure 1(a) and (b). In our article, we have tried to understand the SST–convection relation by studying separately four different regions of the global tropics.

According to Zhang (1993), deep convection in the global tropics is weak and rarely observed where SST is  $< 26^\circ \text{C}$ . Deep convection tends to be more frequent and more intense when it occurs, as SST increases from  $26^\circ \text{C}$  up to  $30^\circ \text{C}$ . At the same time, variability of deep convection relative to constant SST becomes larger with increasing SST. While the surface moisture convergence induced by large-scale SST gradients (Lindzen and Nigam, 1987) promotes large-scale lifting and thereby generation of

\* Correspondence to: Prof. P. V. Joseph, Department of Atmospheric Sciences, Cochin University of Science and Technology, Fine Arts Avenue, Cochin 682016, India. E-mail: porathur@md4.vsnl.net.in

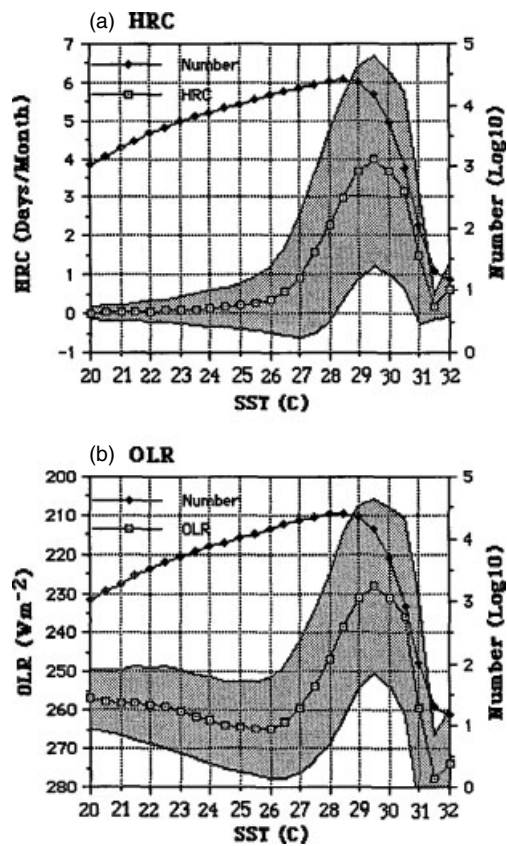


Figure 1. SST–convection relation in the global tropics (reproduced from Waliser *et al.*, 1993) for monthly values in  $2^\circ \times 2^\circ$  latitude–longitude squares of global tropics  $25^\circ\text{S}$  to  $25^\circ\text{N}$  for the period 1975–1985: (a) SST and HRC and (b) SST and OLR. The right vertical axes specify the number of parameter pairs (marked by the line graph) used. It may be noted that very high SST values also have large numbers of the order of  $10^2$  to  $10^3$ . The standard deviation of the means is delineated by the shading.

deep convective clouds, he found that local mean SST is also important for convection. Zang further states that the moisture supply from surface convergence together with fluxes of latent and sensible heat from the warm sea surface into the atmosphere makes conditions favourable for deep convection. He, however, has no explanation for the decrease in convection above SST of  $29^\circ\text{C}$  as observed by Waliser *et al.* (1993).

In regions of large-scale ascending motions in the atmosphere, there is reduction in OLR (increase in deep convection) with respect to increasing SST and the rate of OLR reduction is found to be a strong function of the large-scale motion field (Lau *et al.*, 1997). OLR sensitivity to SST is approximately  $-4$  to  $-5 \text{ W m}^{-2} \text{ C}^{-1}$  in the SST range  $27$ – $28^\circ\text{C}$  under conditions of weak large-scale circulation. Under the influence of strong ascending motion in the atmosphere, this rate can increase to  $-15$  to  $-20 \text{ W m}^{-2} \text{ C}^{-1}$  for the same SST range. They found that there is no threshold of SST like  $29^\circ\text{C}$  beyond which convection decreases with increase in SST. They also found that under the influence of strong large-scale rising motion, convection does not decrease but it increases monotonically with SST even at SST higher than  $29^\circ\text{C}$ .

The reduction in convection observed in high SST situations is likely to be caused by large-scale subsidence forced by nearby or remotely generated deep convection. In central Pacific where the local correlation of SST to OLR is largest, they found that the large-scale circulation has relatively stronger control than local SST on OLR variance. On monthly to inter-annual timescale, they found that 26% of OLR variance is due to SST and 44% due to upper tropospheric divergence.

Deep convection has been shown by a modelling study to be generated by SST gradient in the tropical areas of the Pacific Ocean (Lindzen and Nigam, 1987). SST gradient has been found to be an important forcing mechanism of the low-level tropical flow and convergence. A large fraction of the total convergence in the eastern tropical Pacific is forced by the meridional gradients in SST, whereas in the central and western tropical Pacific, it is the zonal gradients of SST that are the major contributors. They found that the zonal gradients in SST, although smaller than the meridional gradients, can force a response comparable to that forced by the latter. A recent modelling study on the same problem by Back and Bretherton (2009) used a linear mixed layer model, which reproduces observed surface wind and convergence over the tropical oceans. They found that convergence is primarily due to SST gradient and that SST gradient is better regarded as a cause rather than a consequence of deep convection in the tropics.

Shankar *et al.* (2007) found that the meridional gradient of SST in Bay of Bengal during the period mid May to September of 1998–2005 was important for the onset of convection there. They found that the lag between the SST difference (gradient) between south and north Bay of Bengal exceeding  $0.75^\circ\text{C}$  and the onset of convection was less than a week in 75% of the 28 cases studied. Joseph and Sabin (2008) showed that a typical active–break cycle of the Asian summer monsoon begins with maximum SST (at pentad 0 in a composite 8 pentad duration active–break cycle of the Asian summer monsoon) over the north Bay of Bengal. They used Tropical Rainfall Measuring Mission (TRMM) microwave imager (TMI) SST and for convection Geostationary Operational Environmental Satellite (GOES) precipitation index (GPI) rain. An area of organized convection takes genesis over central Bay of Bengal at pentad 1 in the zone of large SST gradient and it pulls the cross-equatorial monsoon low-level jetstream (LLJ) through peninsular India. Convection and the LLJ westerlies then spread to the western Pacific Ocean during the following three pentads. Pentads 1–4 is taken as the active phase of the monsoon during which convection and LLJ have grown in a positive feedback process, as studied by Joseph and Sijikumar (2004).

We have summarized in Section 1 most of the observational studies available to date on the relation between SST and convection in the global tropics. In Section 2, the data used in this study are described. Our observational studies on the relation among SST, surface wind and divergence (and also vertical velocity at 500 hPa)

and convection in the atmosphere on monthly and daily scales, separately for the warm pool areas and the inter-tropical convergence zone (ITCZ)/south Pacific convergence zone (SPCZ) areas of the global tropics, are given in Sections 3 and 4, respectively. Section 5 gives a discussion of the various aspects of SST-convection relation as found in observations. It also draws support for the observed relation from some of the currently available coupled ocean-atmosphere global circulation model (GCM) studies.

## 2. Data used

We used GPI, TMI SST and surface wind from QuikSCAT. One distinct advantage of the TRMM is the onboard microwave imager which gives accurate and reliable SST measurements at high resolution ( $0.25^\circ \times 0.25^\circ$ ) with accuracy of roughly  $0.5^\circ\text{C}$  (Wentz, 1998; Wentz *et al.*, 1998) even in the presence of cloud (Wentz and Schabel, 2000). In our study, we regrid the TMI data to  $1^\circ \times 1^\circ$  grid compatible to the GPI data. Data are available from 1998. The satellite-derived GPI is a good measure of infrared-based daily rainfall estimates on a  $1^\circ \times 1^\circ$  grid of the period 1997 to the present from the global precipitation climatology project products. The one-degree daily precipitation estimation technique is a complete first-generation procedure for estimating global daily precipitation (Huffman *et al.*, 2001).

Two-dimensional surface wind fields (10 m) that were measured by the seawinds scatterometer on the QuikSCAT satellite of the National Aeronautics and Space Agency (Wentz, 1986; Patoux and Brown, 2001) were used to estimate the low-level surface divergence. These data are available only for the period

from June 1999. QuikSCAT was designed to observe wind vectors with an accuracy of  $20^\circ$  in direction and  $2\text{ ms}^{-1}$  in speed and has a spatial resolution of 25 km. These data were also regrid to  $1^\circ \times 1^\circ$  latitude-longitude to be comparable with the GPI data. This high-resolution data set gives a good description of the surface atmospheric circulation field and provides valuable information about the atmospheric conditions over the oceans. Goswami and Rajagopal (2004) made comparisons between the QuikSCAT wind and in situ observations and found that this data set agreed well with the in situ observations for the area studied in our article. We have also used the NCEP-NCAR reanalysed data of vertical velocity at 500 hPa level available on a  $2.5^\circ$  latitude-longitude grid (Kalnay *et al.*, 1996).

## 3. Warm pool SST and the associated convection

### 3.1. Pre-monsoon season in north Indian ocean (16 April to 15 May)

The warm pool over the north Indian ocean is at its highest temperature just before the onset of the Indian summer monsoon over Kerala when this area has the warmest temperature in the global tropics (Joseph, 1990). Maximum SST of the warm pool reaches  $31\text{--}32^\circ\text{C}$  by then. Figure 2(a) gives the TMI SST of the month-long period from 16 April to 15 May averaged for the years 1998–2005. The axis of maximum SST is a north-eastward sloping line whose latitude is about  $2^\circ\text{N}$  in central Arabian Sea and about  $12^\circ\text{N}$  in central Bay of Bengal. The axis of maximum convection as represented by GPI rainfall intensity of the same period (Figure 2(b)) is a few degrees of latitude south of the

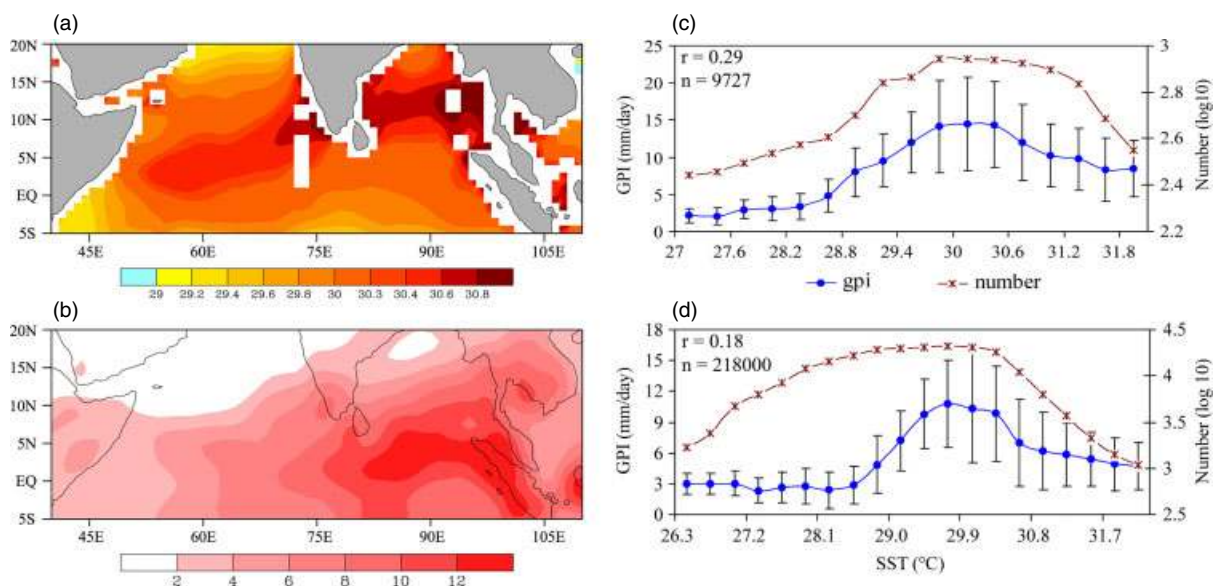


Figure 2. Over north Indian ocean (a) mean TMI SST in  $^\circ\text{C}$  of 16 April to 15 May of 8 years 1998 to 2005. (b) Mean GPI rain fall of the same area and period. The SST-convection relation for data averaged over  $1^\circ$  lat  $\times$   $1^\circ$  long squares. (c) In monthly data and (d) in daily data. Length of the vertical bars represents the standard deviation on either side of the mean. The right vertical axes specify the number of parameter pairs used [in (c) and (d), the linear correlation coefficient and number of observational pairs are marked at top left]. This figure is available in colour online at [wileyonlinelibrary.com/journal/joc](http://wileyonlinelibrary.com/journal/joc)

axis of the warmest SST. It is in an area with large SST gradient, SST increasing to the north. Maximum convective rainfall of 10–14 mm d<sup>-1</sup> is over areas with SST of 29–30°C. The warmest SST axis in the Bay of Bengal has mean temperature of more than 30.6°C, and over this area, the convection is only 6–8 mm d<sup>-1</sup>. In the areas to the north of the SST, maximum convection further decreases. The relation between 1° latitude–longitude square averages of monthly (16 April to 15 May) values (Figure 2(c)) and daily values (Figure 2(d)) of SST and convection (GPI) using data of each year of 1998 to 2005 of the geographical region between latitudes 5°S and 20°N and longitudes 55°E and 95°E (excluding land areas) is very similar to that shown in Figure 1(a) and (b). The linear correlation between SST and convection (marked in the figures), however, is very small in view of the type of SST–convection relation (Waliser type).

The surface (10 m asl) wind is given in Figure 3(a). These are monsoon-type westerlies in response to the convective heating. Joseph and Sijikumar (2004) have shown that for this type of wind (but at 850 hPa), the correlation between convection and wind is maximum and highly significant for a lag of about 2 days, convection leading, showing that the wind is a delayed response to the convective heating of the atmosphere. The divergence of the surface wind is shown in Figure 3(b). It is seen that the active convection area (Figure 2(b)) is where the divergence is negative (convergence). This is also the area of large SST gradient (Figure 2(a)). The central area of the warm pool (of maximum SST) has positive divergence. The divergence–convection relation for monthly data is shown in Figure 3(c). The linear

correlation between them is large. Convection is found to increase steadily with increase in convergence for all values of divergence. Figure 3(d) gives the relation between vertical velocity at 500 hPa and convection and the linear correlation between them is also very high (the vertical velocity used is taken from NCEP reanalysis, Kalnay *et al.*, 1996), which is on 2.5° × 2.5° grid. Therefore, for this figure, GPI data were also reduced to this grid.

### 3.2. Monsoon season in northwest Pacific Ocean (July and August)

The SST of the warm pool over the northwest Pacific Ocean is very high during the Asian summer monsoon period. The SST–convection relation in this area during July and August is analysed. SST of the warm pool reaches 30–31°C during these months. Figure 4(a) gives the mean TMI SST of the period 1 July to 31 August of the years 1998 to 2005. The axis of maximum SST is along latitude of about 18°N. The axis of maximum convection as represented by GPI rainfall intensity of the same period (Figure 4(b)) is a few degrees of latitude south of the axis of the warmest SST. The area of high convection (GPI) is where SST gradient is large, SST increasing to the north. Convective rainfall of 14–20 mm/d is over areas with SST around 29.5°C. The warmest SST axis over the west Pacific Ocean has temperatures of more than 30.2°C, and over this area, the convection is <12 mm d<sup>-1</sup>. In the areas to the north of the SST, maximum convection decreases rapidly. The relation between 1° latitude–longitude square averages of monthly and daily values of SST and convection of the period 1 July to 31 August using data of each year of

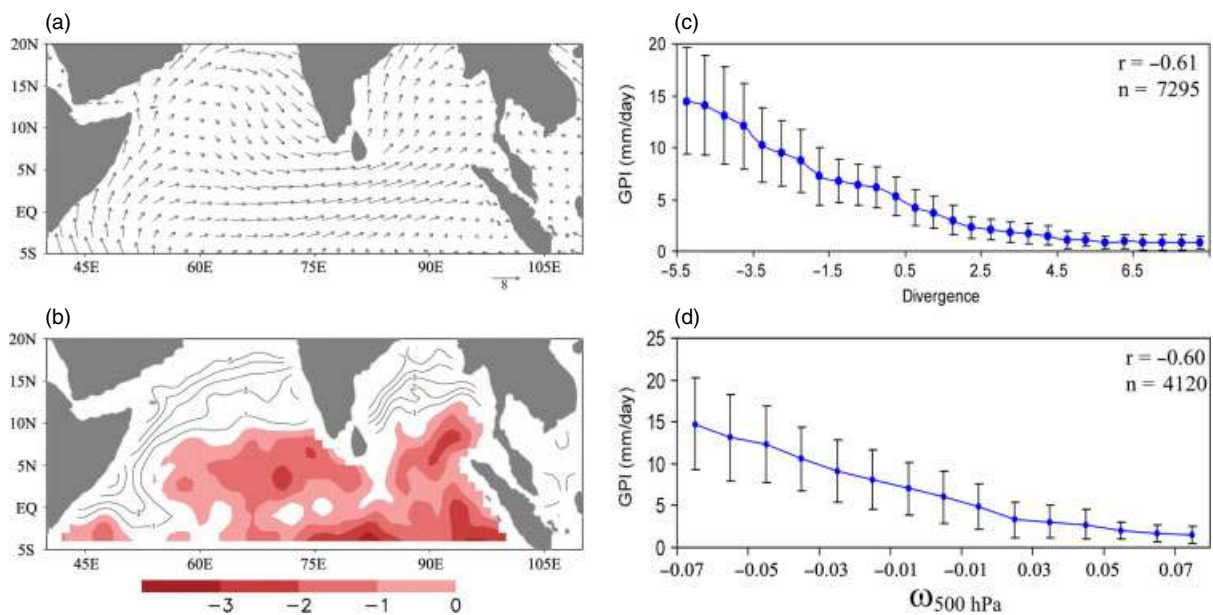


Figure 3. Over north Indian ocean (a) mean QuikSCAT wind ms<sup>-1</sup> of 16 April to 15 May of 6 years 2000 to 2005. (b) Divergence of the wind given at (a) in 10<sup>-6</sup> s<sup>-1</sup>. (c) Divergence–convection (GPI) relation in monthly data averaged over 1° lat × 1° long squares and (d) vertical velocity at 500 hPa–convection (GPI) relation in monthly data averaged over 2.5° lat × 2.5° long. Vertical bars are as in Figure 2 [in (c) and (d), the linear correlation coefficient and number of observational pairs are marked at top right]. This figure is available in colour online at [wileyonlinelibrary.com/journal/joc](http://wileyonlinelibrary.com/journal/joc)

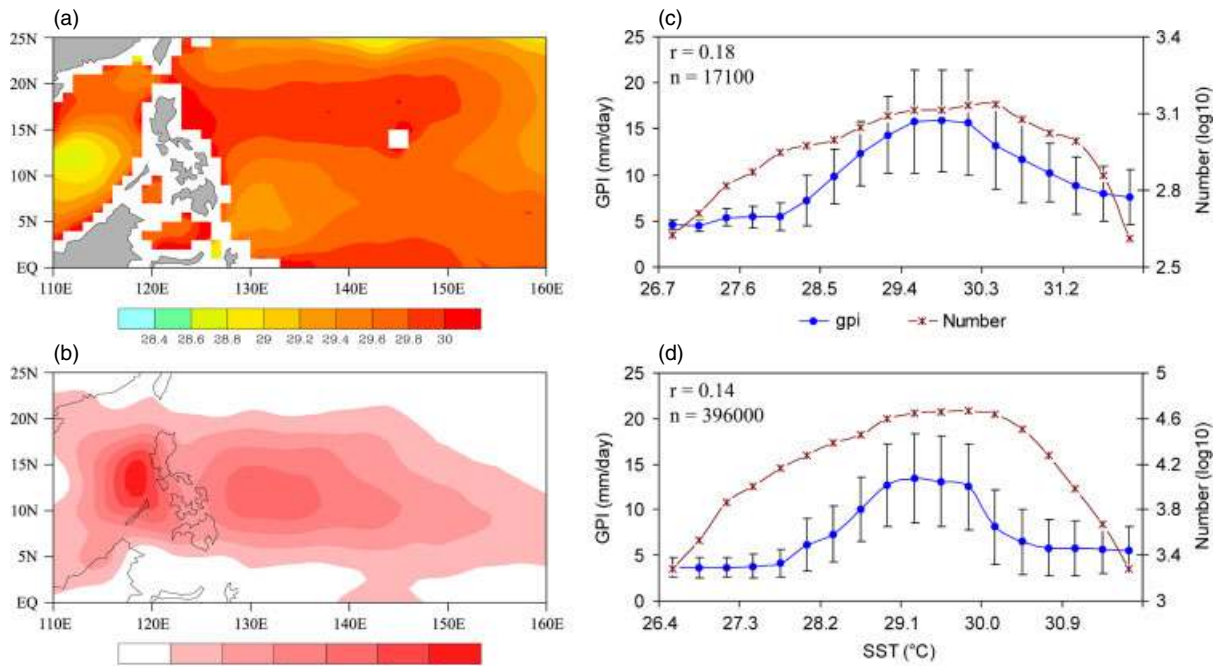


Figure 4. Over northwest Pacific Ocean (a) mean TMI SST in  $^{\circ}\text{C}$  of July and August of 8 years 1998 to 2005. (b) Mean GPI rain fall of the same period. (c) SST-convection relation in monthly data and (d) SST-convection relation in daily data [in (c) and (d), the linear correlation coefficient and number of observational pairs are marked at top left. Vertical bars and number of observations are as in Figure 2. The data in (c) and (d) are averages over  $1^{\circ}$  lat  $\times$   $1^{\circ}$  long squares]. This figure is available in colour online at [wileyonlinelibrary.com/journal/joc](http://wileyonlinelibrary.com/journal/joc)

1998–2005 of the geographical region between latitudes  $0^{\circ}\text{N}$  and  $25^{\circ}\text{N}$  and longitudes  $110^{\circ}\text{E}$  and  $160^{\circ}\text{E}$  are shown in Figure 4(c) and (d), respectively. These figures are very similar to Figure 1(a) and (b). SST data cover a large span from  $26.4$  to  $31.8^{\circ}\text{C}$ . The convection begins to increase at SST of  $27.8^{\circ}\text{C}$ , reaches maximum values at  $29.0$ – $29.8^{\circ}\text{C}$  and decreases for higher temperatures. It is noted that these ranges are higher for the north Indian ocean for the period 16 April to 15 May. In the case of north west Pacific Ocean also, the linear correlation between SST and convection (as marked in the figure) is small.

The surface wind (10 m asl) is given in Figure 5(a). These are monsoon-type westerlies in the latitude belt  $5^{\circ}\text{N}$  to  $15^{\circ}\text{N}$ . That the convection–wind relation is as per the Joseph and Sijikumar (2004) finding has been shown for this area by Joseph and Sabin (2008), convection leading the wind by about 2 days. The divergence of the surface wind is shown in Figure 5(b). It is seen that the active convection area is where the divergence is negative (convergence). This is also the area of large SST gradient. As in the case of the north Indian ocean basin, the linear correlation between divergence and convection is large and statistically significant. The divergence–convection relation for monthly data is shown in Figure 5(c). Convection is found to increase with increase in convergence for all divergence–convergence values. Figure 5(d) gives the distribution of GPI as a function of vertical velocity at 500 hPa level. The near linear increase in convection with vertical velocity is clear from this figure. The high linear correlation values (shown in figure) between them is statistically significant.

#### 4. SST and convection over ITCZ and SPCZ areas

##### 4.1. ITCZ over the northeast Pacific Ocean (July and August)

During the months of July and August, there is a convectively active ITCZ over northeast Pacific Ocean where the convection is particularly vigorous during El-Nino years. The mean SST of July and August of the period 1998–2005 is given in Figure 6(a). Maximum of convection is found to be collocated with areas of maximum SST (Figure 6(b)), unlike in the two cases discussed in Section 3 where maxima of convection occurred in areas of large SST gradient. The SST–convection relation using the monthly and daily  $1^{\circ}$  latitude–longitude square averages of SST and convection of the period 1 July to 31 August using data of each year of 1998–2005 of the geographical region between latitudes  $5^{\circ}\text{S}$  and  $25^{\circ}\text{N}$  and longitudes  $160^{\circ}\text{E}$  and  $100^{\circ}\text{W}$  are given in Figure 6(c) and (d), respectively. Convection is found to increase with SST for all values of SST very much different from the Waliser *et al.* (1993) model given in Figure 1(a) and (b). SST data have varied from  $22.5$  to  $31^{\circ}\text{C}$ . Convection begins at a SST of  $26.5^{\circ}\text{C}$  and reaches maximum values at the maximum SST. The linear correlation between SST and convection is high unlike for the warm pool cases. In the case of the ITCZ, convection is found to increase monotonically with SST even at SSTs higher than  $29^{\circ}\text{C}$  (non-Waliser type).

The wind at 10 m level in response to the ITCZ convective heating is given in Figure 7(a) and the divergence in Figure 7(b). Relation between monthly values of divergence and convection (GPI) are shown in Figure 7(c)

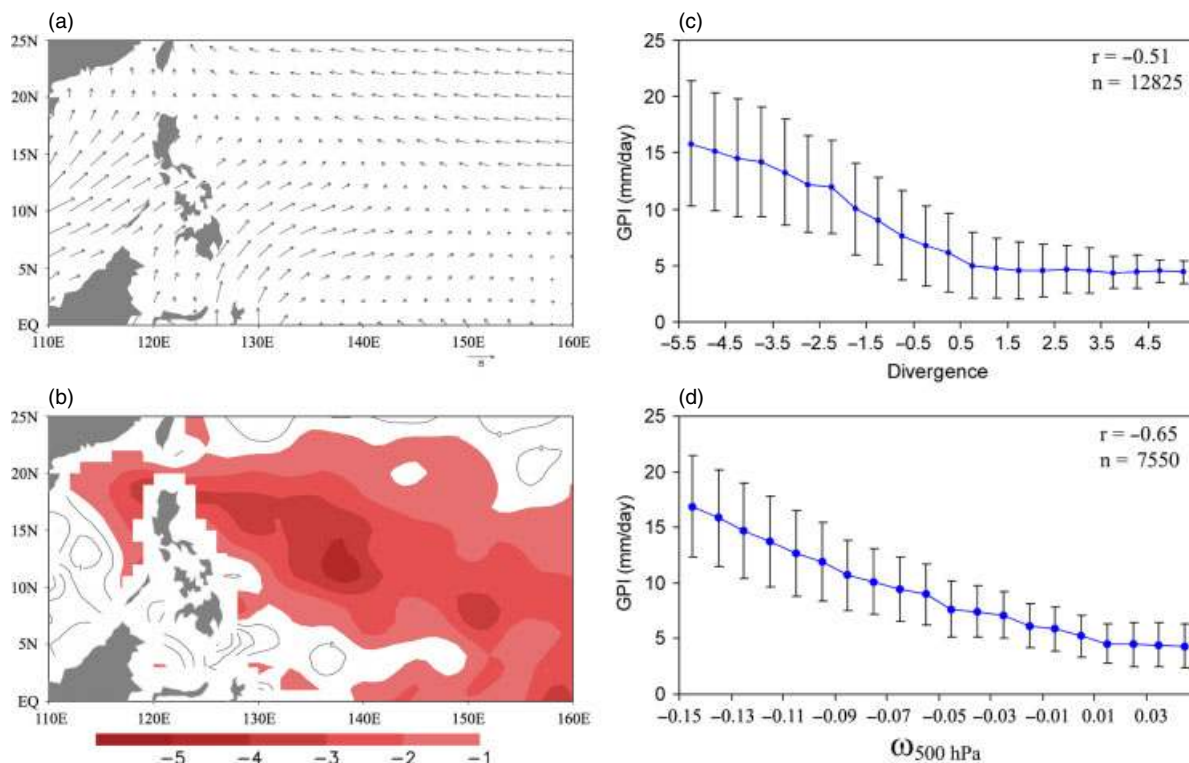


Figure 5. Over northwest Pacific Ocean (a) mean QuikSCAT wind  $\text{ms}^{-1}$  of July and August of 6 years 2000 to 2005. (b) Divergence of the wind given at (a) in  $10^{-6} \text{ s}^{-1}$ . (c) Divergence–convection relation in monthly data and (d) vertical velocity at 500 hPa–convection relation in monthly data. Vertical bars are as in Figure 2 [in (c) and (d), the linear correlation coefficient and number of observational pairs are marked at top right. The data in (c) are averages over  $1^\circ \text{ lat} \times 1^\circ \text{ long}$  squares and those in (d) are averages over  $2.5^\circ \text{ lat} \times 2.5^\circ \text{ long}$  squares]. This figure is available in colour online at [wileyonlinelibrary.com/journal/joc](http://wileyonlinelibrary.com/journal/joc)

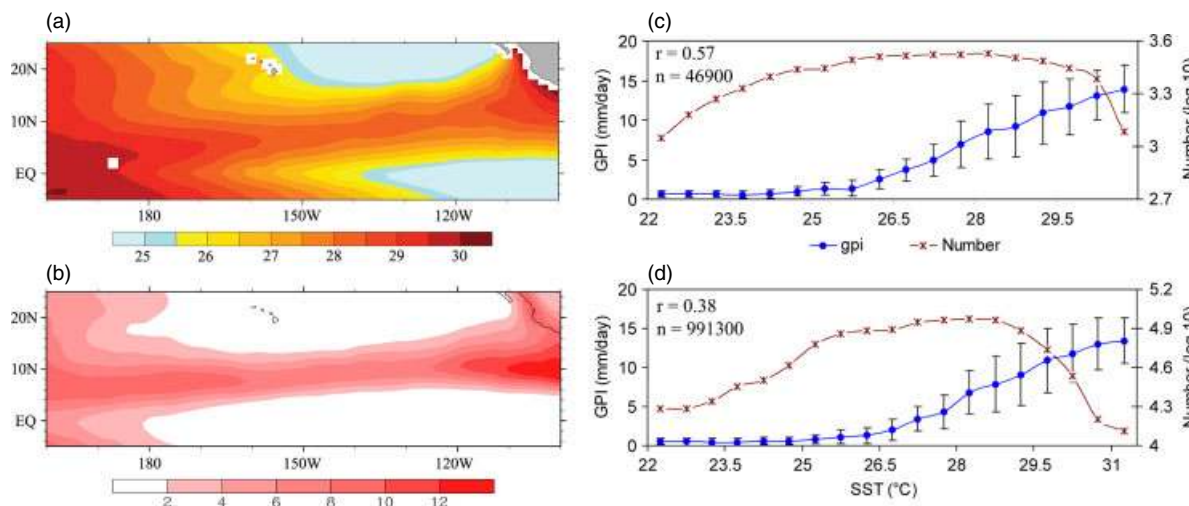


Figure 6. Over the ITCZ area of east Pacific Ocean (a) mean TMI SST in  $^\circ\text{C}$  of July and August of 8 years 1998 to 2005. (b) Mean GPI rainfall of the same period. (c) SST–convection relation in monthly data and (d) SST–convection relation in daily data. Vertical bars and number of observations are as in Figure 2 [in (c) and (d), the linear correlation coefficient and number of observational pairs are marked at top left. The data in (c) and (d) are averages over  $1^\circ \text{ lat} \times 1^\circ \text{ long}$  squares]. This figure is available in colour online at [wileyonlinelibrary.com/journal/joc](http://wileyonlinelibrary.com/journal/joc)

(data in  $1^\circ \times 1^\circ$  grid) and the relation between vertical velocity at 500 hPa and convection in Figure 7(d) (data in  $2.5^\circ \times 2.5^\circ$  grid). In the ITCZ case, the linear correlations between convection and SST, convection and divergence and convection and 500 hPa vertical velocity are all high and statistically significant (correlation values are marked in the figures).

Examination of Figure 6(a) and (b) has shown two special features.

- (a) In the longitude belt  $160^\circ\text{E}$  to  $130^\circ\text{W}$ , the maxima of SST and convection coincide, but in the portion  $130^\circ\text{W}$  to  $100^\circ\text{W}$ , the active convection area is south of the latitude of maximum SST as in the

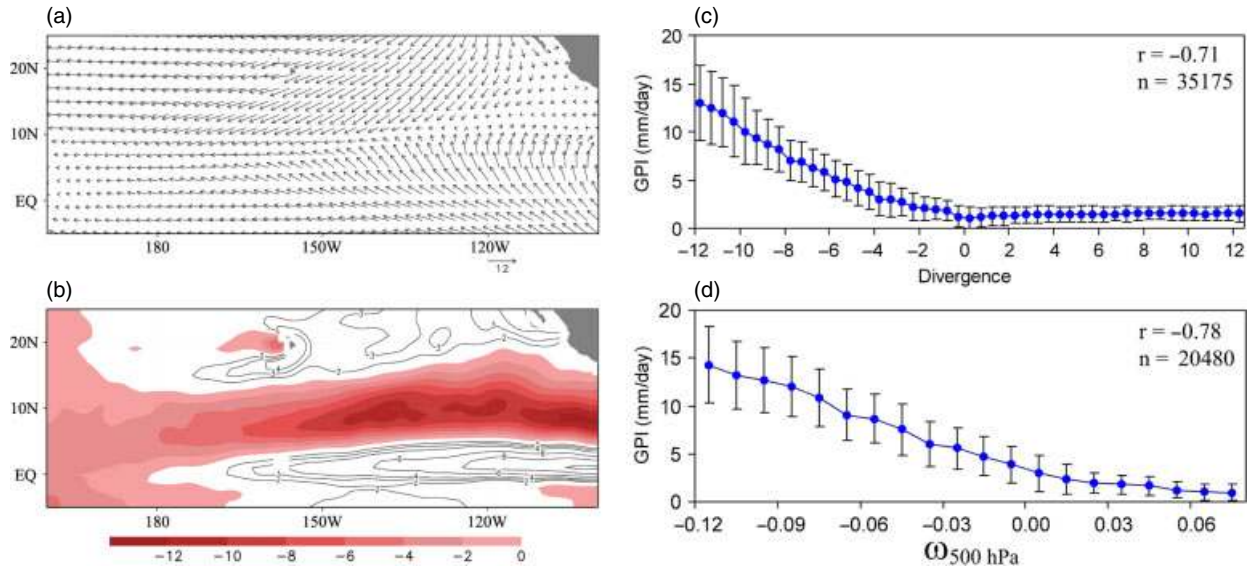


Figure 7. Over the ITCZ area of east Pacific Ocean (a) monthly mean QuikSCAT wind  $\text{ms}^{-1}$  of July and August of 6 years 2000 to 2005. (b) Divergence of the wind given at (a) in  $10^{-6} \text{ s}^{-1}$ . (c) Divergence-convection relation in monthly data and (d) vertical velocity at 500 hPa-convection relation in monthly data. Vertical bars are as in Figure 2 [in (c) and (d), the linear correlation coefficient and number of observational pairs are marked at top right. The data in (c) are averages over  $1^\circ \text{ lat} \times 1^\circ \text{ long}$  squares and those in (d) are averages over  $2.5^\circ \text{ lat} \times 2.5^\circ \text{ long}$  squares]. This figure is available in colour online at [wileyonlinelibrary.com/journal/joc](http://wileyonlinelibrary.com/journal/joc)

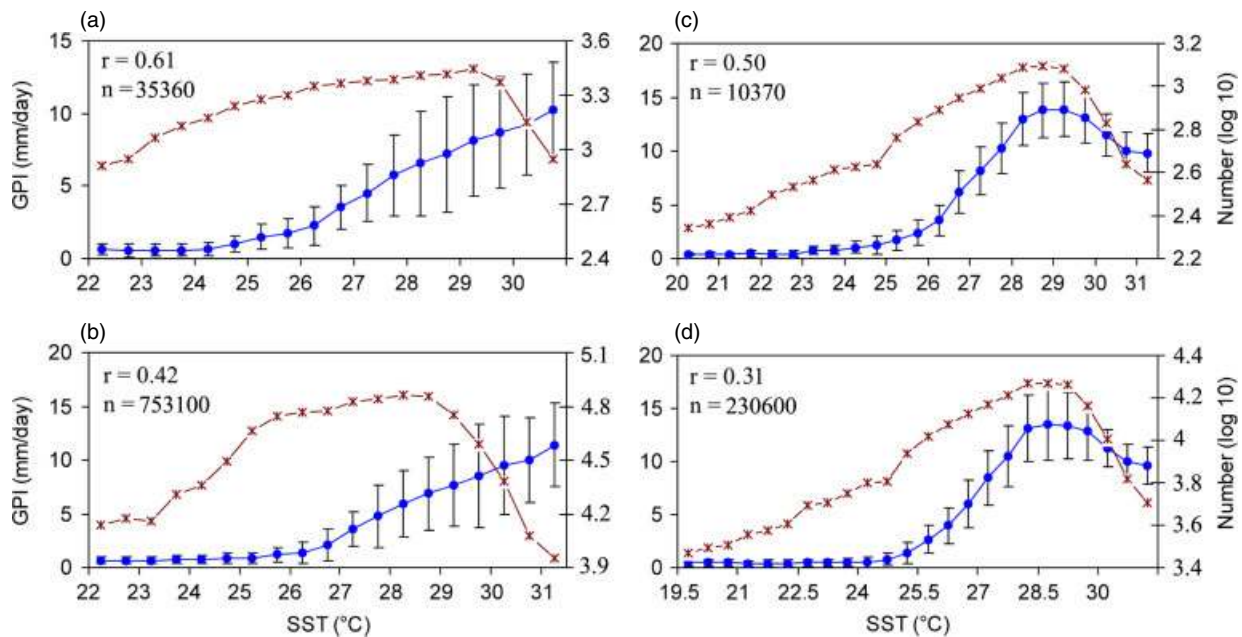


Figure 8. SST-convection relation in monthly (a) and daily (b) data of the  $1^\circ \text{ lat}$ -long bins of area  $160^\circ\text{E}$ - $130^\circ\text{W}$ ,  $5^\circ\text{S}$ - $25^\circ\text{N}$ . (c) and (d) give the same for  $130^\circ\text{W}$ - $100^\circ\text{W}$ ,  $5^\circ\text{S}$ - $25^\circ\text{N}$ . Vertical bars and number of observations are as in Figure 2 (the linear correlation coefficient and number of observational pairs are marked at top left). This figure is available in colour online at [wileyonlinelibrary.com/journal/joc](http://wileyonlinelibrary.com/journal/joc)

case of the warm pool areas of Indian and western Pacific Oceans. This part of the Pacific Ocean in July and August is a monsoon area (the north American monsoon). We examined the SST convection relation for these two subareas and the results are given in Figure 8(a)-(d) for the monthly and daily scales. The SST-convection relation is of the warm pool or monsoon or Waliser type for the eastern portion (close to the North American continent) of the north Pacific ITCZ. However, for the portion of the east

Pacific between the longitudes  $160^\circ\text{E}$  and  $130^\circ\text{W}$ , the SST-convection relation is of the non-Waliser type.  
 (b) The western side of the east Pacific ITCZ box  $160^\circ\text{E}$ - $130^\circ\text{W}$  has high SST, high convection and low convergence. The eastern part of the box has low SST, high convergence and low convection. The multiple correlation between the three parameters for this box is 0.82 (the linear correlation between SST and convection is 0.57, that between convection



Table I. Linear correlation coefficient between SST and convection, divergence and convection and SST and divergence and the multiple correlation coefficient between these parameters for the four different areas of the global tropics studied (using monthly data).

	Correlations <sup>a</sup>			
	SST-GPI <sup>b</sup>	Div-GPI <sup>b</sup>	SST-Div	Multiple CC
North Bay (16 Apr–15 May)	0.29	−0.61	−0.12	0.64
W Pacific (Jul–Aug)	0.18	−0.51	−0.15	0.52
ITCZ (Jul–Aug)	0.57	−0.71	−0.24	0.82
SPCZ (Jan–Feb)	0.59	−0.72	−0.51	0.76

<sup>a</sup> All correlation values are significant at 99.9% by *t*-test.

<sup>b</sup> GPI rain stands for convection.

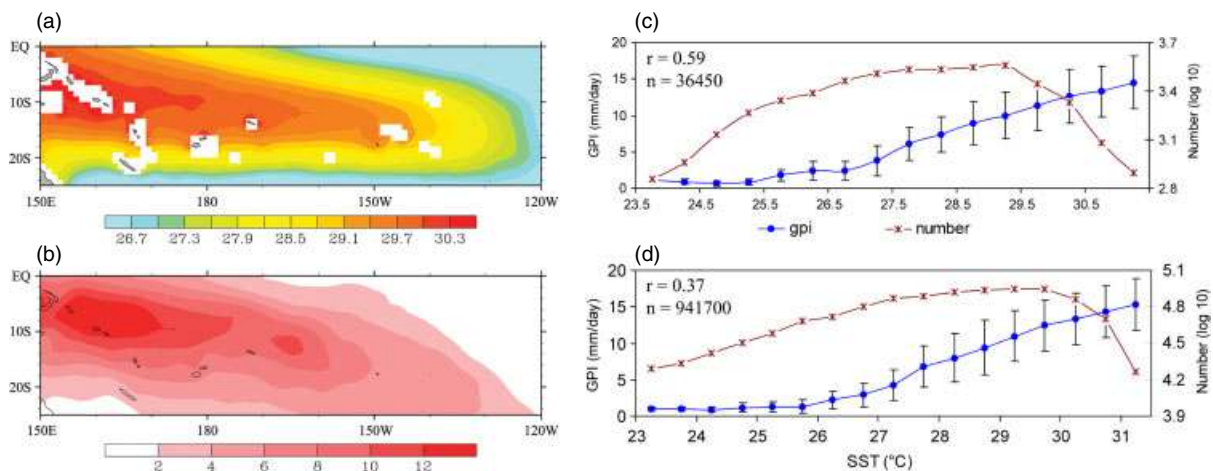


Figure 9. Over the SPCZ area of west Pacific Ocean (a) mean TMI SST in °C of January and February of 8 years 1998 to 2005. (b) Mean GPI rain of the same period. (c) SST–convection relation in monthly data and (d) SST–convection relation in daily data. Vertical bars and number of observations are as in Figure 2 [in (c) and (d), the linear correlation coefficient and number of observational pairs are marked at top left. The data in (c) and (d) are averages over  $1^\circ$  lat  $\times$   $1^\circ$  long squares]. This figure is available in colour online at [wileyonlinelibrary.com/journal/joc](http://wileyonlinelibrary.com/journal/joc)

and convergence is  $-0.71$  and that between SST and convergence is only  $-0.24$ ). Similar correlation values for all the four regions studied are given in Table I.

#### 4.2. SPCZ over the southwest Pacific Ocean (January and February)

There is an active SPCZ over southwest Pacific Ocean during January and February (Vincent, 1994). We have studied the SST–convection relation of the SPCZ area during these two months of 1998–2005. The axis of maximum SST is located near latitude  $10^\circ$ S and extends from longitudes  $150^\circ$ E to  $120^\circ$ W (Figure 9(a)). The area of maximum convection as represented by GPI rainfall intensity of the same period (Figure 9(b)) is located around the axis of maximum SST. In this case also as in the case of the ITCZ, convection is found to increase with SST for all values of SST. Convection begins to increase at SST of  $27.5^\circ$ C, increases with SST and reaches maximum values at the maximum SST in the SPCZ area. The relation between  $1^\circ$  latitude–longitude square averages of monthly and daily values of SST and convection of the months January and February using data of each year of 1998–2005 of the geographical region between

the equator and latitude  $25^\circ$ S and longitudes  $150^\circ$ E and  $120^\circ$ W are shown in Figure 9(c) and (d), respectively. Convection increases monotonically with SST even at SST higher than  $29^\circ$ C. The 10 m-level wind in response to the SPCZ convective heating is given in Figure 10(a) and the divergence in Figure 10(b). Relation between monthly values of divergence and convection (GPI) are shown in Figure 10(c) (data in  $1^\circ \times 1^\circ$  grid) and the relation between vertical velocity at 500 hPa and convection in Figure 10(d) (data in  $2.5^\circ \times 2.5^\circ$  grid). In the SPCZ case, the linear correlations between convection and SST, convection and divergence and convection and 500 hPa vertical velocity are all very high.

### 5. Summary and discussions

This study has shown that SST–convection relation over the warm pool regions of Indian and west Pacific Oceans (monsoon areas) has convection increasing with SST in the SST range  $26$ – $29^\circ$ C, and for SST higher than  $29^\circ$ C, convection decreases with increase in SST. We call this the Waliser type of SST–convection relation (Waliser *et al.*, 1993). An explanation for this type of SST–convection relation has been offered invoking the

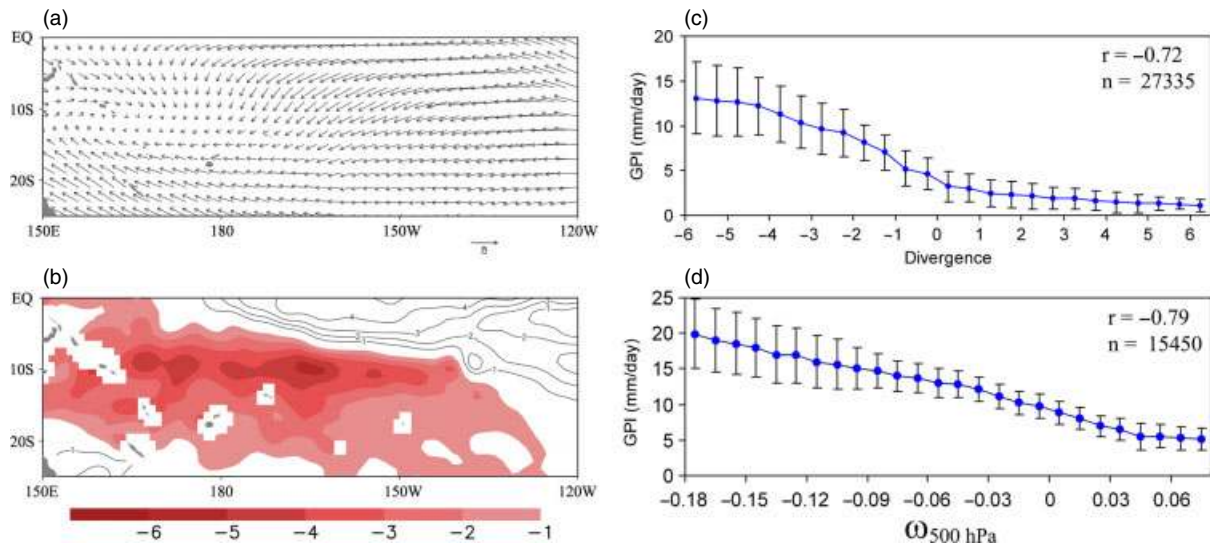


Figure 10. Over the SPCZ area of west Pacific Ocean (a) monthly mean QuikSCAT wind  $\text{ms}^{-1}$  of January and February of 6 years 2000 to 2005. (b) Divergence of the wind given at (a) in  $10^{-6} \text{ s}^{-1}$ . (c) Divergence–convection relation in monthly data and (d) vertical velocity at 500 hPa–convection relation in monthly data. Vertical bars are as in Figure 2 [in (c) and (d), the linear correlation coefficient and number of observational pairs are marked at top right. The data in (c) are averages over  $1^\circ \text{ lat} \times 1^\circ \text{ long}$  squares and those in (d) are averages over  $2.5^\circ \text{ lat} \times 2.5^\circ \text{ long}$  squares]. This figure is available in colour online at [wileyonlinelibrary.com/journal/joc](http://wileyonlinelibrary.com/journal/joc)

modelling studies by Lindzen and Nigam (1987) and Back and Bretherton (2009), which has shown that convection is related to SST gradient in the tropical ocean. That convection is induced in areas with SST gradients has been shown through data analysis for the warm pool areas of Indian and west Pacific Oceans (1) by Joseph *et al.* (2006) in the case of monsoon onset over India and (2) by Vecchi and Harrison (2002) and Joseph and Sabin (2008) in the case of active–break cycle of the monsoon. As described in Section 1, Shankar *et al.* (2007) have shown that convection sets over the Bay of Bengal during the summer monsoon season within a week after the SST difference between north and south Bay of Bengal exceeds  $0.75^\circ\text{C}$ . Once deep convection is initiated in the SST gradient area south of the central region of the warm pool, the deep tropospheric heating by the latent heat released in the convective clouds produces strong low-level wind fields particularly cross-equatorial LLJ on the equatorward side of the warm pool and both the convection and LLJ are found to grow through a positive feedback mechanism (Joseph and Sijikumar, 2004; Joseph and Sabin, 2008). Thus, SST through its gradient acts only as an initiator of convection. Large values of convection are associated with the cyclonic vorticity of the LLJ in the atmospheric boundary layer (which for low-latitude areas having low values of coriolis parameter produces large values of convergence and vertical upward motion of the moist air mass there). The prevailing conditionally unstable atmosphere in the tropics is favourable for the production of deep convective clouds. Since the central region of the warm pool has very small SST gradients, large amounts of deep convection cannot be generated there. We are thus giving a thermodynamic cum dynamic explanation for the observed relation (Waliser type) between SST and

convection associated with a warm pool region whose central area is located away from the equator.

A question arises here as to the role of SST in the generation of deep convection. Graham and Barnett (1987) showed that convection depends on both SST and divergence in the atmosphere. Lau *et al.* (1997) through a detailed statistical analysis for the tropics found that on monthly to interannual timescale, 26% of the variance of convection is due to SST and a much larger percentage (44%) is due to divergence in the atmosphere. It is known that deep convection occurs in areas having large values of convective available potential energy (CAPE) and it is also known that the temperature of the lowest 1–2 km of the atmosphere has a direct relation to the magnitude of CAPE. The air temperature of this atmospheric layer is closely linked to the underlying SST because of turbulent mixing in the atmospheric boundary layer. Vertical upward motion due to divergence in the atmosphere (negative divergence in the lower troposphere or positive divergence in the upper troposphere) is a necessary factor to raise the warm and moist lower tropospheric air to levels above the level of free convection to release the CAPE stored in the atmosphere for the production of deep convection, which might explain the dependence of convection on SST and divergence.

In the cases of the warm pool studied in this article, the linear correlation coefficient (LCC) between SST and convection is small as the high SST areas (central region of warm pool) have very low convection. This LCC, however, is statistically significant, which confirms the observed weak dependence of convection on SST. For these cases, the LCC between the low-level divergence obtained from QuikSCAT winds and the convection is very high, showing the stronger dependence

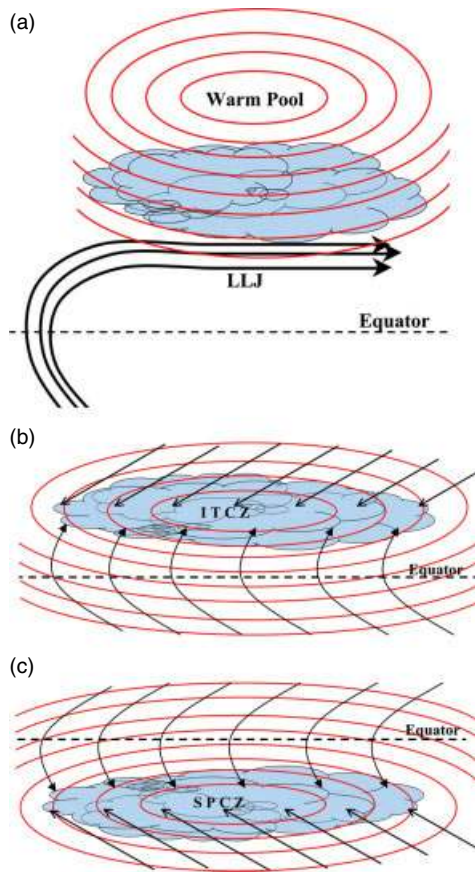


Figure 11. Schematic diagram showing the relation between SST, convection, wind flow and LLJ in (a) warm pool, (b) ITCZ and (c) SPCZ areas. SST isotherms marked show areas of maximum SST. Areas of convection are shaded. This figure is available in colour online at [wileyonlinelibrary.com/journal/joc](http://wileyonlinelibrary.com/journal/joc)

of convection on low-level convergence, which is related to the vertical motion in the atmosphere. This is again confirmed by the finding that vertical velocity at 500 hPa is also having high LCC with convection.

In contrast are the cases of ITCZ and SPCZ in which the SST maxima are located close to the equator (latitudes 5°–10°) where the axes of maximum SST nearly coincide with the axes of maximum convection in the monthly

means. Boundary layer air streams from the north and south hemispheres converge along the axis of maximum SST in monthly means (they have slightly different latitudinal positions on a day-to-day basis). For these cases, we found that the LCC between convection and SST, convection and divergence (obtained from QuikSCAT winds) and convection and vertical velocity at 500 hPa are all very high. Thus, in the cases of ITCZ and SPCZ, the relation between SST and convection is not of the Waliser type; instead, convection increases with SST for all values of SST. Schematic diagrams showing the isotherms of SST, streamlines of wind flow and LLJ, wind convergence zones and the areas of convection are given in Figure 11(a)–(c) for the warm pool, ITCZ and SPCZ cases discussed in this article. Figure 11(b) and (c) for the ITCZ and SPCZ, respectively, are mirror images.

Some of the available modelling studies support the purely observational findings of this study. The characteristics of the summer monsoon climate over south Asia, east Asia and the western north Pacific Ocean (monsoon areas) were studied using the Meteorological Research Institute-coupled GCM (MRI-CGCM2) by Rajendran *et al.* (2004). The relationship between SST and convection in the model outputs as obtained by them is of Waliser type as can be seen from Figure 12 (their Figure 3(a)). SST–convection relation has been reproduced satisfactorily in their modelling study over the entire range of SSTs, including the reduction in convection for high SSTs (above 29 °C).

We examined the 100 year runs of the Intergovernmental Panel on Climate Change Fourth Assessment Report (IPCC-AR4)-coupled ocean–atmosphere models of the climate of the twentieth century (20c3m) simulations. The simulated convection of the MPI ECHAM5 model (Jungclaus *et al.*, 2006) for the ITCZ and SPCZ areas is in good agreement with the observed SST–convection relation as obtained by us. Figure 13(a) gives the SST (shaded) and convection (contour) for the 100 year mean of the simulation (1900–1999) of the MPI ECHAM model (both the parameters reduced to the same grid size of 2° lat × 2° lon for the east Pacific ITCZ. It is seen

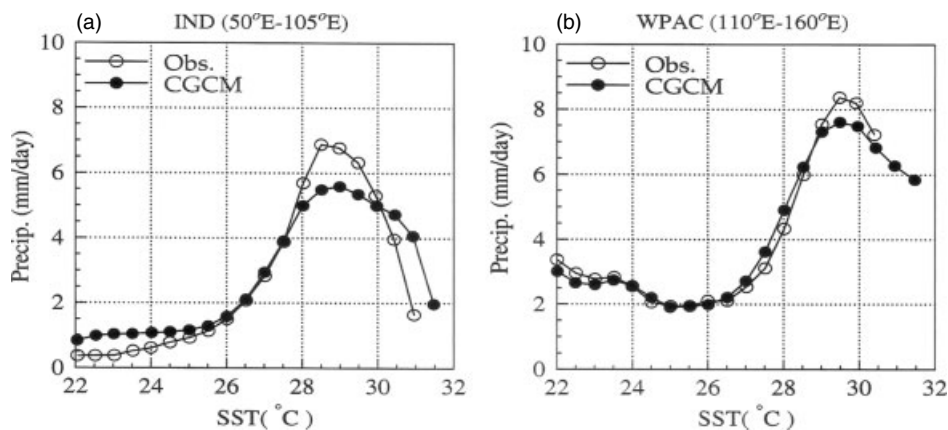


Figure 12. SST–convection relation in the global tropics – in the observations and in a coupled ocean-atmosphere model (MRI-CGCM2) are given in (a) for the Indian ocean tropics and (b) for the west Pacific tropics for June to September period (reproduced from Rajendran *et al.*, 2004).

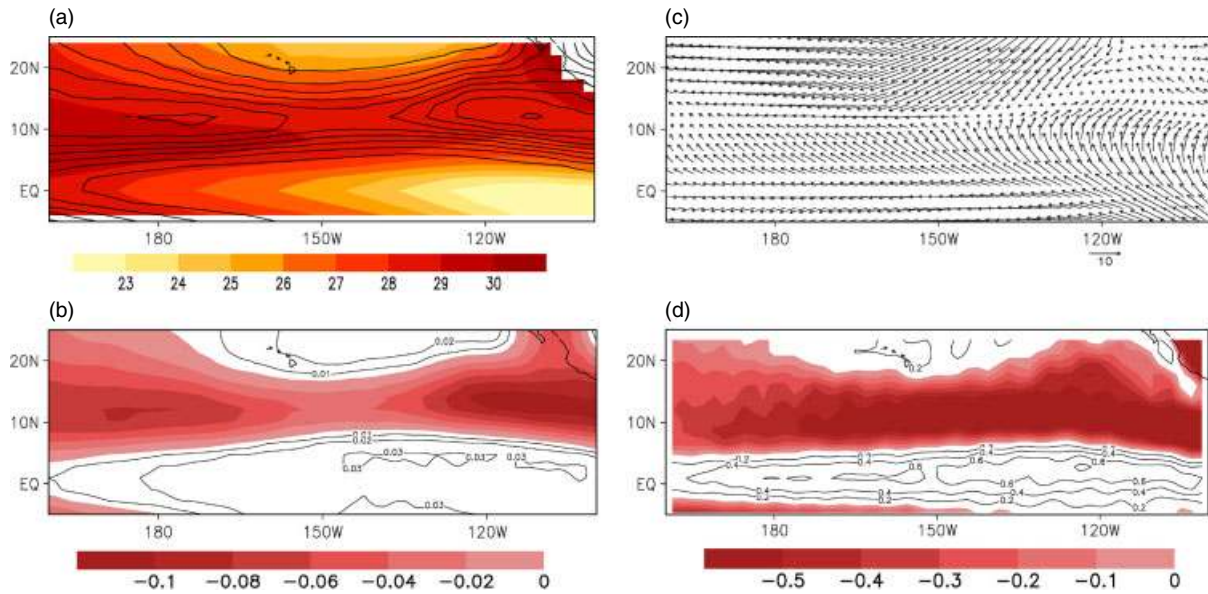


Figure 13. Over the ITCZ area of east Pacific Ocean MPI ECHAM5 simulated. (a) Monthly mean SST (shaded) and precipitation (contour) of July and August of 100 years 1900 to 1999. (b) Vertical velocity at 500 hPa. (c) Monthly mean surface wind in  $\text{ms}^{-1}$ . (d) Divergence of the wind given in  $10^{-6} \text{ s}^{-1}$ . This figure is available in colour online at [wileyonlinelibrary.com/journal/joc](http://wileyonlinelibrary.com/journal/joc)

that the relationship between SST and convection in the model outputs is of the non-Walser type for the area west of longitude  $130^{\circ}\text{W}$  and of the Walser type for the area east of  $130^{\circ}\text{W}$  as in observations (see descriptions in Section 4.1). This is further confirmed by Figure 14(a) and (b), which gives the relation between monthly values of modelled SST and modelled convection for the ITCZ area (divided into two parts). Simulations by three more ocean-atmosphere-coupled models (IPCC runs) studied (GFDL Cm2.0, GFDL Cm2.1 and UKMO Had Gem models) also show non-Walser type of SST-convection relation for ITCZ/SPCZ areas.

The difference in the SST-convection relation between the summer monsoon warm pool areas and the ITCZ areas as discussed in this article has been noted by Webster *et al.* (1998) in their Figure 25. They have also given an explanation for the observed difference in the SST-convection relation between these two areas in their Section 3.4. Relation between SST and convection is very important in the field of numerical modelling of tropical rainfall. It is well known that models generally do rainfall simulation very well in ITCZ but are found unable to do satisfactory simulation in the monsoon areas. Observational studies as presented in this article are hoped to lay the ground work for developing better modelling studies.

### Acknowledgements

The authors thank the editor and the anonymous referees for their constructive suggestions and comments to improve the article. TPS thank Dr. R Krishnan, Executive Director, CCCR for all encouragements and Prof. BN Goswami, Director, IITM for extending all support for this research work. IITM is fully funded by Ministry

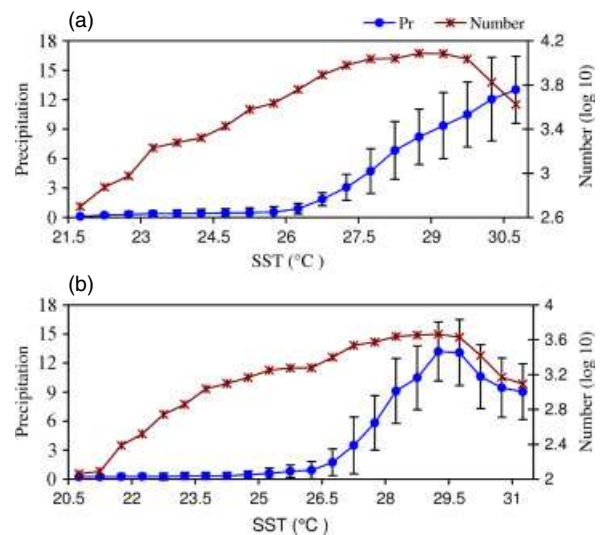


Figure 14. MPI ECHAM5 simulated, SST-convection relation in monthly data for July and August of 1900 to 1999 of ITCZ area in  $2^{\circ}$  latitude-longitude bins (a)  $160^{\circ}\text{E}-130^{\circ}\text{W}$ ,  $5^{\circ}\text{S}-25^{\circ}\text{N}$ . (b) gives the same for  $130^{\circ}\text{W}-100^{\circ}\text{W}$ ,  $5^{\circ}\text{S}-25^{\circ}\text{N}$ . Vertical bars and number of observations are as in Figure 2. This figure is available in colour online at [wileyonlinelibrary.com/journal/joc](http://wileyonlinelibrary.com/journal/joc)

of Earth Science, Govt. of India. The authors are also thankful to the Indian Space Research Organization for funding this Research Project under the MOP program of their Space Application Center, Ahmedabad. Department of Atmospheric Sciences, CUSAT, is thanked for providing facilities and support to do this research. One of the authors (T.P.S.) is thankful to the University Grants Commission of India (Research Fellowship in Sciences for Meritorious Students) for financial support during part of the research period. We acknowledge the modelling groups, for providing their data for analysis, the Program

for Climate Model Diagnosis and Intercomparison and WCRP's Working Group on Coupled Modelling for their roles in making available the WCRP CMIP3 multi-model data set. The IPCC data archive at the Lawrence Livermore National Laboratory is supported by the Office of Science, the US Department of Energy. The authors are thankful to Dr. Tim Palmer of ECMWF for his suggestion to use IPCC-AR4 model outputs in support of our empirical relation between SST and convection.

## References

- Back LE, Bretherton CS. 2009. On the relationship between SST gradients boundary layer winds and convergence over the tropical oceans. *Journal of Climate* **22**: 4182–4196.
- Bjerknes J. 1966. A possible response of the atmospheric Hadley circulation to equatorial anomalies of ocean temperature. *Tellus* **18**: 820–829.
- Bjerknes J. 1969. Atmospheric Teleconnections from the equatorial Pacific. *Monthly Weather Review* **97**: 163–172.
- Gadgil S, Joseph PV, Joshi NV. 1984. Ocean-atmosphere coupling over monsoon regions. *Nature* **312**: 141–143.
- Goswami BN, Rajagopal EN. 2004. Indian Ocean surface winds from NCMRWF analysis as compared to QuikSCAT and moored buoy winds. *Proceedings of Indian Academy of Sciences (Earth and Planetary Sciences)* **112**: 61–77.
- Graham NE, Barnett TP. 1987. Sea surface temperature, surface wind divergence, and convection over tropical ocean. *Science* **238**: 657–659.
- Huffman GJ, Adler RF, Morrissey MM, Bolvin DT, Curtis S, Joyce R, Mcgavock B, Susskind J. 2001. Global precipitation at one degree daily resolution from multisatellite observations. *Journal of Hydro Meteorology* **2**: 36–50.
- Joseph PV. 1990. Monsoon variability in relation to equatorial trough activity over Indian and west Pacific Oceans. *Mausam* **2**: 291–298.
- Joseph PV, Sabin TP. 2008. An ocean-atmosphere interaction mechanism for the active break cycle of the Asian summer monsoon. *Climate Dynamics* **30**: 553–566. DOI: 10.1007/s00382-007-0305-2.
- Joseph PV, Sijikumar S. 2004. Intra seasonal variability of the low level jet stream of the Asian summer monsoon. *Journal of Climate* **17**: 1449–1458.
- Joseph PV, Sooraj KP, Rajan CK. 2006. The summer monsoon onset process over south Asia and an objective method for the date of monsoon onset over Kerala. *International journal of Climatology* **26**: 1871–1893.
- Jungclaus JH, Botzet M, Haak H, Marotzke J, Mikolajewicz U, Roeckner E, Keenlyside N, Latif M, Luo JJ. 2006. Ocean circulation and tropical variability in the AOGCM ECHAM5/MPI-OM. *Journal of Climate* **19**: 3952–3972.
- Kalnay EM, Kanamitsu M, Kistler R, Collins W, Deaven D, Gandin L, Iredell M, Saha S, White G, Woollen J, Zhu Y, Leetmaa A, Reynolds R, Chelliah M, Ebisuzaki W, Higgins W, Janowiak J, Mo KC, Ropelewski C, Wang J, Jenne R, Joseph D. 1996. The NCEP/NCAR 40 year reanalysis project. *Bulletin of the American Meteorological Society* **77**(3): 437–471.
- Lau KM, Wu HT, Bony S. 1997. The role of large scale atmospheric circulation in the relationship between tropical convection and sea surface temperature. *Journal of Climate* **10**: 381–392.
- Lindzen RS, Nigam S. 1987. On the role of sea surface temperature gradients in forcing low-level winds and convergence in the tropics. *Journal of Atmospheric Sciences* **44**: 2418–2436.
- Patoux J, Brown RA. 2001. A scheme for improving scatterometer surface wind fields. *Journal of Geophysical Research* **106**: 23995–24005.
- Rajendran K, Kitoh A, Yukimoto S. 2004. South and east Asian summer monsoon climate and variation in the MRI coupled model (MRI-CGCM2). *Journal of Climate* **17**: 763–782.
- Shankar D, Shetye SR, Joseph PV. 2007. Link between convection and meridional gradient of sea surface temperature in the Bay of Bengal. *Proceedings of Indian Academy of Sciences (Earth and Planetary Sciences)* **116**: 385–406.
- Vecchi GA, Harrison DE. 2002. Monsoon breaks and sub seasonal sea surface temperature variability in the Bay of Bengal. *Journal of Climate* **15**: 1485–1493.
- Vincent DG. 1994. The south Pacific convergence zone (SPCZ): a review. *Monthly Weather Review* **122**: 1949–1970.
- Waliser DE, Graham NE, Gautier C. 1993. Comparison of the highly reflective cloud and outgoing longwave data sets for use in estimating tropical deep convection. *Journal of Climate* **6**: 331–353.
- Webster PJ, Magana VO, Palmer TN, Shukla J, Tomas RA, Yanai M, Yasunari T. 1998. Monsoons: processes predictability and the prospects for prediction. *Journal of Geophysical Research* **103**: 14451–14510.
- Wentz FJ. 1986. Users manual SEASAT scatterometer wind vectors. RSS Technical Report, 081586, Remote Sensing Systems, Santa Rosa, CA, 21pp.
- Wentz FJ. 1998. Algorithm theoretical basis document: AMSR ocean algorithm. Remote Sensing System Technical Report, 110398, Santa Rosa, 65.
- Wentz FJ, Gentemann C, Smith D, Chelton D. 1998. Satellite measurements of sea surface temperature through clouds. *Science* **288**: 847–850.
- Wentz FJ, Schabel M. 2000. Precise climate monitoring using complementary satellite data sets. *Nature* **403**: 414–416.
- Zhang C. 1993. Large scale variability of atmospheric deep convection in relation to sea surface temperature in the tropics. *Journal of Climate* **6**: 1898–1913.